

COB-2023-0253

EVALUATION OF FLOW BOILING PRESSURE DROP AT HIGH MASS VELOCITIES IN A SINGLE MICROCHANNEL USING R123

Thalles Coimbra Borba Roldão

Juliana Silva Brasil

Cristiano Bigonha Tibiriçá

Heat Transfer Research Group, Escola de Engenharia de São Carlos, Universidade de São Paulo, São Carlos, SP, Brazil

thalles.roldao@usp.br

juliana.brasil@usp.br

bigonha@sc.usp.br

Abstract. This paper presents new experimental data on pressure drop during convective boiling in microchannels. The tests were conducted in a single stainless steel microchannel with an internal diameter of 1.1mm, a heated length of 100mm, and a total length of 210mm. High mass velocities of 2000 and 2500 kg/m²s were used. The working fluid approached was R123, which has a potential for use in applications such as Organic Rankine Cycles. The data may be used, as well, to compare the pressure drop of R123 with other new fluids that shall replace it in the next years. The objective of this paper is to evaluate the predicted values of pressure drop with the experimental data. During calculations, it is necessary to use a frictional pressure drop correlation and a void fraction correlation, so the error associated with each correlation has an influence on the final result. The correlation of void fraction is used in the prediction of the acceleration component. Three correlations for void fraction and as many frictional pressure drop correlations for two-phase flow available in the literature were selected. In order to evaluate the influence of both kinds of correlations in the predicted values, they were combined, resulting in nine different combinations. The experimental values were compared to the results of each combination. The results show that all combinations have had similar and good results in the prediction of the pressure drop. Although the acceleration parcel of the pressure drop is sometimes neglected, the void fraction correlation has had an important influence on the results.

Keywords: Flow Boiling, Pressure Drop, Microchannels, High mass velocity, R123

1. INTRODUCTION

The promotion of intense heat exchange in small-sized components is a prominent area in the development and research of heat transfer in mechanical engineering. The reduction in the size of electronic components that need to be cooled is one of the factors that have expanded the application of convective boiling in microchannels (Lombaard *et al.* (2021)), among several other applications such as the organic Rankine cycle, (Ennio and Marco (2017)), refrigeration and aerospace industry (Hall and Mudawar (1999)), automobile industry, heating, nuclear and solar energy (Ribatski *et al.* (2006)).

One of the most important parameters in the design of a heat exchanger or heat sink based on microchannels with convective boiling is the pressure drop. In these cases, the pressure drop can be very high and make some small-scale applications unfeasible because they require larger and more powerful flow machines. Therefore, the correct prediction of pressure drop during flow boiling is essential. The pressure drop of two-phase flow is related to three main components: the pressure drop due to friction, the pressure drop due to gravitational effects, and the pressure drop related to change in flow velocity due to the phase change, boiling, or condensation, as explained by Kanizawa and Ribatski (2021).

The pressure drop due to gravitational and momentum variation effects, called acceleration in the literature, can be calculated by theoretical models available in the literature. In the case of the accelerational pressure drop, the void fraction must be calculated. To obtain the void fraction, empirical correlations may be needed depending on the conditions of the flow. Some models are available in the literature, the main ones being the slip ratio model and the drift flux model. Some correlations of the first model are those of Tibiriçá *et al.* (2017) and Gardenghi *et al.* (2020), besides the theoretical homogeneous model, which is applicable only under conditions of very low or high vapor qualities. The drift flux model correlations are based on the work of Zuber and Findlay (1965), which laid the foundation for this model. Derived correlations followed, such as the one by Rouhani (1969). Other models were proposed such as the one of Kanizawa and Ribatski (2016), which considers a condition of minimum momentum flux along the cross-section of the flow to develop a relation for the void fraction.

The two-phase frictional pressure drop needs to be calculated using empirical correlations. Different correlation

models exist, such as the homogeneous model, based on average properties between the liquid and gas phases, and the two-phase multiplier model, which obtains the two-phase loss by multiplying the pressure drop that the flow would have if it were single-phase by an adjustment factor.

Examples of frictional pressure drop correlations are that of Cicchitti *et al.* (1960) and Tibiriçá *et al.* (2017) for the homogeneous model. For the two-phase multiplier model, some examples are those of Lockhart and Martinelli (1949), Chisholm (1973), Friedel (1979), and Kim and Mudawar (2014). One of the most used and cited in the literature is the correlation of Müller-Steinhagen and Heck (1986), originally proposed as a relation between the pressure drop of the flow as liquid and as vapor, it can also be presented as a two-phase multiplier model. Other models consider the flow pattern in the prediction of the frictional pressure drop, such as the correlation of Quibén and Thome (2007).

Studies about the flow boiling pressure drop of pure R123 were presented in the literature. Hardik and Prabhu (2018) collected data for a helical coil with tube diameters of 5.5 to 9.5 mm. Mass velocities between 141 and 1421 kg/m²s were used. Tank *et al.* (2021) studied flow boiling of R123 in a horizontal tube with 11.9 mm of external diameter and used mass velocities between 180 to 1210 kg/m²s. However, there is a lack of studies about the pressure drop of R123 during flow boiling in microchannels. It is worth mentioning that, in this paper, it is considered that microscale phenomena occur for tubes with internal diameters smaller than 3 mm, as indicated by Kandlikar (2010). Only one study relating results for this condition was found, proposed by Okajima *et al.* (2018). These authors have applied flow boiling in a microstructure of 0.07 and 0.08mm internal diameter with applications related to medical devices. A few pressure drop data were presented by the authors.

It is relevant to obtain more data about the flow boiling of R123 so that its performance may be compared to new low-pressure fluids and mixtures that might replace it. Beyond that, R123 is still produced and may be used yet in applications such as the organic Rankine cycle, as indicated by Pang *et al.* (2017). In this context, the aim of this paper is to present new experimental data on pressure drop during convective boiling of R123 in a microchannel, to contribute to data banks for this fluid. High mass velocities of 2000 and 2500 kg/m²s were used. This range is rarely present in the literature for R123, as reviewed by (Roldão *et al.* (2022)). Beyond that, predictive methods of frictional pressure drop and void fraction correlation were evaluated in predicting experimental values. Three different frictional pressure drop correlations and three void fraction correlations were tested. The pressure drop prediction was conducted by combining each frictional pressure drop correlation with each void fraction correlation, in order to include the influence of both in the results since the void fraction prediction is necessary when calculating the accelerational parcel of the pressure drop. The performance of each combination was analyzed by mean absolute error and by data convergence within a 20% error range.

2. EXPERIMENTAL APPARATUS AND PROCEDURE

The experimental apparatus is represented in Fig. 1. It consists of a refrigerant circuit with a pump, a DC power source to promote boiling, a condenser, a subcooler, and a reservoir. Other components as a filter, a Coriolis mass flow meter, and a bypass valve are present. Starting from the pump the fluid flows to the test section, where the DC power source applies a current directly on the external surface of the tube to promote the boiling of the fluid. The test section is made of a unique horizontal stainless-steel microchannel with a 1.1 mm internal diameter 1.3 mm of external diameter, and 100 mm of heated length. The total length of the microchannel is 210mm. Downstream the test section the fluid is directed to the condenser, formed by a tube-in-tube heat exchanger. Upstream the condenser, the fluid passes through a subcooler, whose function is to ensure that the fluid will enter the pump in a subcooled condition, to avoid cavitation. Upstream the subcooler the fluid passes through a filter and downstream the fluid enters the pump. A cooled water circuit is also present in the experimental apparatus, although it is not represented in Fig. 1. The cooled water is used in the condenser and in the sub-cooler to exchange and absorb heat from the working fluid.

A Coriolis mass flow meter is positioned between the subcooler and the pump. The desired mass flow rate is set up by a frequency controller acting on the pump and by a bypass piping line containing a needle valve that is installed between the inlet and the outlet of the pump. The bypass also ensures the system's security. Insulation materials are used across the whole piping to prevent heat exchange with the environment.

Just upstream the test section, the enthalpy of the liquid is estimated from its temperature by a thermocouple located at an adiabatic position on the outside tube wall, and its pressure by an absolute pressure transducer. Just downstream the test section another thermocouple located at an adiabatic position measures the outlet fluid temperature, which is taken as the reference saturation temperature, and the outlet pressure is measured by another absolute pressure transducer. The location of the thermocouples on the test section can be seen in Fig.2.

The experiments were conducted first by setting the mass velocity through the frequency controller acting on the pump. Then heat was applied to the test section to initiate the boiling. The heat flux was progressively increased by incrementing the electrical current in small steps, letting the temperatures and pressures stabilize. This procedure was repeated at each mass velocity tested. Labview was used to collect all the data and to control the system.

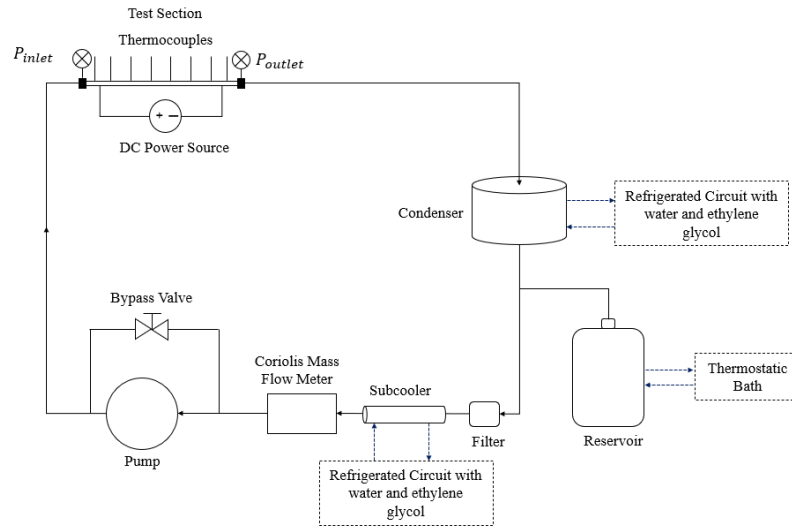


Figure 1. Experimental Apparatus.

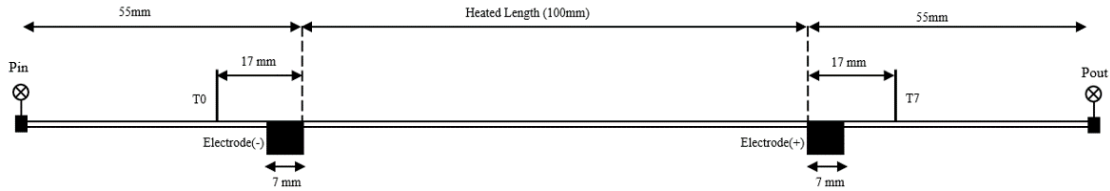


Figure 2. Test Section.

3. DATA REDUCTION

The equations used in this study are described in this topic. The variables present in this paper are the mass velocity (G), the thermodynamic vapor quality (x), the saturation temperature of the fluid (T_{sat}) and its pressure drop (ΔP). The mass velocity is given by the ratio between the mass flow (\dot{m}) and the cross-sectional area of the pipe used, as shown in Eq.(1), in which, D is the internal tube diameter.

$$G = \frac{\dot{m}}{\frac{\pi D^2}{4}} \quad (1)$$

The thermodynamic vapor quality is measured along the flow and is calculated by an energy balance along the channel, as in Eq. (2). The enthalpies of saturated liquid (h_{sl}) and vaporization (h_{fg}) are functions of the local pressure along the flow. The calculation of local pressure is explained later in this topic. The calculation of enthalpies from local pressures was performed using the EES (Klein and Alvarado (2020)) software. The vapor quality is also a function of the inlet enthalpy of the fluid (h_{in}), the heat flux applied (q''), the internal tube diameter, the mass velocity, and the position, z , along the tube.

$$x(z) = \frac{h_{in} + \frac{q'' \pi D z}{G \pi D^2 / 4} - h_{sl}(z)}{h_{fg}(z)} \quad (2)$$

The heat flux applied (q'') was calculated with Eq. (3), which is dependent on the electrical current (I) and tension (U) applied, and the heat exchange area, calculated with the internal tube diameter (D) and heated length (L_h).

$$q'' = \frac{U.I}{\pi D L_h} \quad (3)$$

The flow reference saturation temperature is agreed as the temperature at the end of the boiling section and was experimentally obtained in this study by the thermocouple located at the microchannel outlet, indicated by T_7 in Fig. 2. The experimental pressure drop is obtained by the difference between the pressures read by the pressure transducers at the microchannel outlet and inlet, illustrated in Fig. 2.

The experimental total pressure drop was obtained by subtracting the inlet pressure from the outlet pressure, measured with the low-uncertainty pressure transducers, as in Eq. (4). And the total pressure gradient was calculated by the ratio of the total pressure drop to the total length of the tube (L), as in Eq. (5).

$$\Delta P = P_{outlet} - P_{inlet} \quad (4)$$

$$\left(\frac{dP}{dz}\right)_{total} = \frac{\Delta P_{total}}{L} \quad (5)$$

The calculation of the pressure drop, and the local pressure along the flow, is done through a discretized analysis of the flow in the microchannel. Figure 3 illustrates the experimental behavior of the flow. Along the microchannel, there is a region where fluid heating occurs and two adiabatic regions, immediately before and after the heating section. Single-phase flow is present along the first adiabatic region and at the beginning of the heating region. Then the convective boiling starts, characterizing the two-phase flow. Boiling develops until the end of the heating region, after which the second adiabatic region follows. In this part of the flow, the fluid is already in a saturation condition and, due to the pressure drop in the flow, the evaporation of the fluid continues by flash effect, since the tube is insulated.

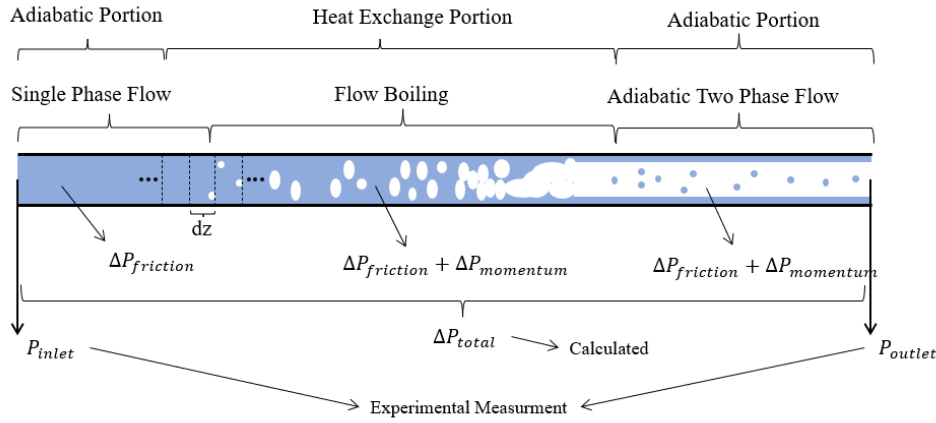


Figure 3. Flow scheme

In the single-phase flow region, the pressure drop is related to the frictional losses and this was calculated with Eq. (6), using the friction factor (f) given by the Pethukov correlation (1970), as in Eq. (7), and dependent on the Reynolds number, calculated with Eq. 8. In these equations, ρ is the density, and μ is the viscosity of the liquid refrigerant.

In the two-phase region, there is a frictional pressure drop and an accelerational pressure drop. Gravitational pressure drop was not present since the tube was positioned horizontally. Frictional pressure drop is calculated using correlations. As part of the objective of this article is to analyze the performance of frictional two-phase correlations, 3 different correlations found in the literature were used to analyze this pressure drop component. The correlations are those of Friedel (1979), Muller-Steinhagen and Heck (1986), and Tibiriçá et al. (2017).

$$\left(\frac{dP}{dz}\right)_{sp} = \frac{2fG^2}{D\rho} \quad (6)$$

$$f = (0.079 \ln(Re) - 1.64)^{-2} \quad (7)$$

$$Re = \frac{GD}{\mu} \quad (8)$$

The accelerational pressure gradient, $\left(\frac{dP}{dz}\right)_a$ can be calculated using a theoretical model given by Eq. (9) (Kanizawa and Ribatski (2021)). In this equation, α is the void fraction, a parameter that is also calculated through correlations. To evaluate the effect of void fraction correlations, 3 models available in the literature were used: Rouhani (1969), Kanizawa and Ribatski (2016), and Tibiriçá et al. (2017).

$$\left(\frac{dP}{dz}\right)_a = G^2 \frac{d}{dz} \left[\frac{(1-x)^2}{\rho_l(1-\alpha)} - \frac{x^2}{\rho_g\alpha} \right] \quad (9)$$

A code was implemented to perform the discretization and calculate all the pressure drop components in each element of the flow. The accelerational pressure drop was calculated iteratively, using Eq. 9, employing a method indicated by Kanizawa and Ribatski (2021). A length of 1 mm was considered for each discretization element.

For each experimental point, nine values for the pressure drop in the tests were obtained with the implemented code. Each of these values is the result of combining one of the three selected frictional pressure drop correlations with one of the three selected void fraction correlations. The comparison between the calculated and experimental values indicates which of the combinations used presented the best correspondence with the experimental data.

The Mean Absolute Error was used to evaluate the performance of the predictive methods. It is calculated as indicated in Eq. (10), in which n is the number of measurements made.

$$MAE = \frac{\sum_{i=1}^n \frac{|Measured - Predicted|}{Measured}}{n} \quad (10)$$

4. EXPERIMENTAL VALIDATION AND UNCERTAINTIES

The uncertainties of the experimental measurements are shown in Tab. 1. The uncertainties in measuring the diameter (D), heated length (L), temperatures (T), and mass flow (\dot{m}) were obtained with information from the manufacturers. The uncertainty of the mass velocity (G), vapor quality (x), the heat supplied (Q_s) by the direct current source and the heat exchanged (Q_f) by the fluids in the single-phase tests were calculated through the propagation of uncertainties, using the software EES (Klein and Alvarado (2020)).

Table 1. Experimental Uncertainties

Parameter	Uncertainty	Parameter	Uncertainty
D	0.02 mm	G	<0.377%
L, L_h	1 mm	x	<3.52%
\dot{m}	0.1%	T	0.15°C
P	2.1 kPa	Q_f	<6.35%
ΔP	3.1 kPa	Q_s	<0.32%
q''	<2.1%		

Single-phase tests were conducted to validate the pressure drop measurement by comparing them with calculated values. The results are displayed in Fig. 4. As can be seen in the figure, the error between the experimental and calculated measurements was less than about 15%. It is observed that the error tended to be smaller from head losses of about 25 kPa, which is precisely the range of the experimental results analyzed in this article. The average absolute error of these tests was 12.51% and a smaller error occurs for data with head loss greater than 25 kPa. These results were considered satisfactory.

Single-phase tests to validate the energy balance in the flow were also conducted and the results are shown in Fig. 5. The power supplied to the flow was compared with the calculated one. The error tended to be smaller the higher the flow rate used, which is expected. The results indicate a deviation within a 10% margin, which was considered satisfactory for being within the uncertainty.

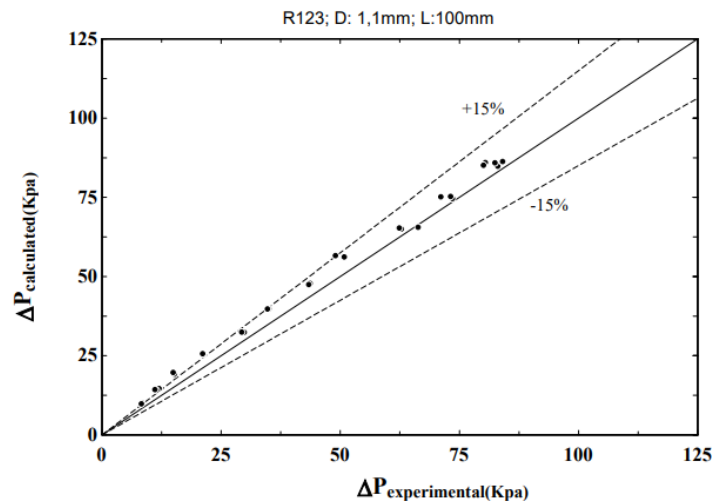


Figure 4. Pressure Drop Validation

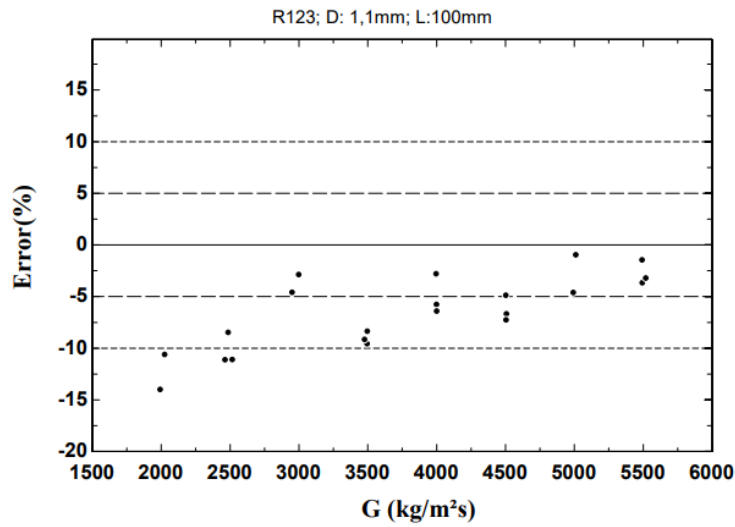


Figure 5. Energy Balance Validation

5. EXPERIMENTAL RESULTS

The experimental points obtained are shown in Tab. 2 and Fig. 6. All results were obtained with R123 in a tube with 100 mm of heating section, 210 mm in total length, and 1.1 mm in diameter. The mass flow rates used were 2000 and 2500 kg/m². The pressure drop of the points obtained was between about 25 and 200 kPa. There was a single-phase section at the beginning of the test section, so the pressure drop in the two-phase section was obtained by subtracting the single-phase pressure drop from the total measured pressure drop and the two-phase length was calculated with the discretized code by calculating the flow length with vapor quality higher than zero. These results are also shown in Tab. 2. The degree of subcooling ($\Delta T_{sub,in}$) in the inlet of the channel is also indicated in the Table. Figure 6 shows the pressure drop as a function of the vapor quality at the tube outlet.

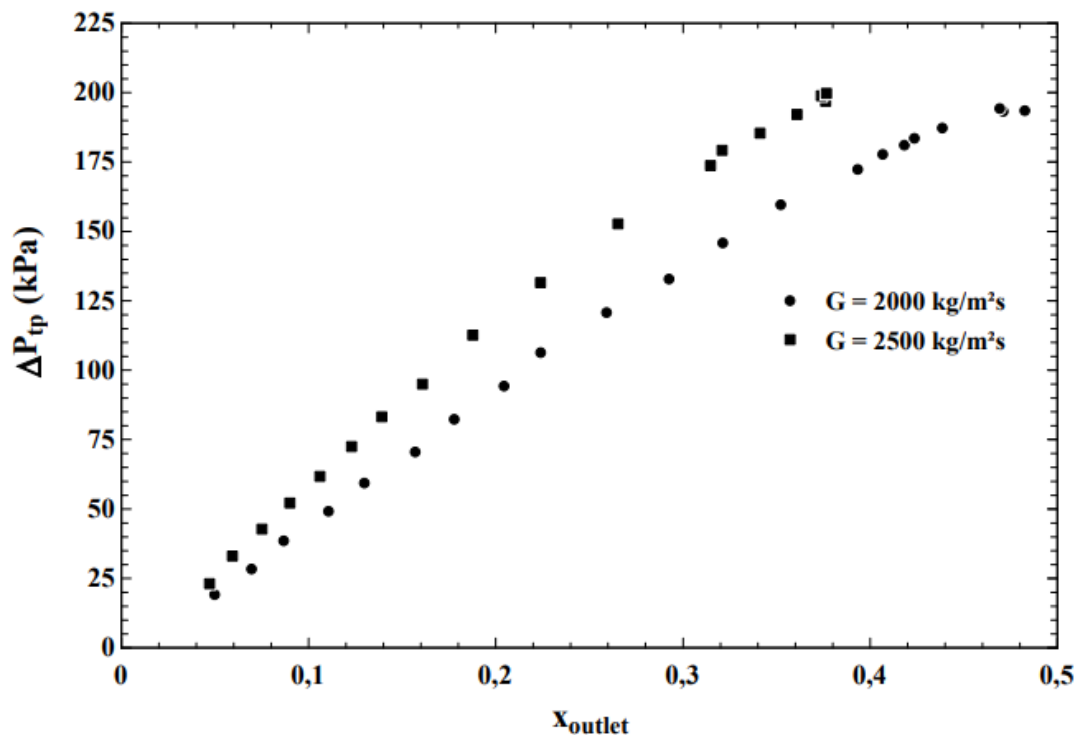


Figure 6. Experimental Two-Phase Pressure Drop versus vapor quality

The comparison between the experimental results and the calculated values for the pressure drop can be analyzed in Tab. 3 and 4. The first one presents the MAE error obtained with each combination and Tab. 4 brings the percentage of

Table 2. Experimental Two-phase Pressure Drop Data

N ^o	(dP) _{total} (kPa)	(dP/dz) _{total} kPa/m	(dP/dz) _{ip} kPa/m	G kg/m ² s	T _{sat} °C	x _{out} (-)	q'' kW/m ²	ΔT _{sub,in} °C
1	25.5	121.43	242.9	2001	39.15	0.05	109.14	15
2	34.34	163.52	333.9	1987	40.56	0.069	128.36	16,36
3	44.44	211.62	437.7	2018	41.68	0.087	149.07	17,44
4	54.7	260.48	528.9	1984	42.98	0.111	171.48	18,7
5	64.93	309.19	631.9	2010	44.29	0.13	195.69	19,95
6	75.75	360.71	720.1	1974	45.79	0.157	221.57	21,4
7	87.58	417.05	832.1	2000	47.34	0.178	249	22,93
8	99.35	473.1	933.6	1991	49.06	0.205	278.18	24,58
9	111.6	531.43	1043.1	2034	50.78	0.224	309	26,25
10	125.7	598.57	1150.5	1999	52.52	0.259	341.41	27,93
11	137.6	655.24	1241.1	1979	54.32	0.293	375.64	29,67
12	150.5	716.67	1350.0	1994	56.02	0.321	411.53	31,32
13	164.4	782.86	1465.1	2009	57.71	0.352	449.19	32,93
14	176.9	842.38	1553.2	1988	59.41	0.393	488.31	34,54
15	182.4	868.57	1601.8	2006	60.25	0.407	508.61	35,33
16	185.6	883.81	1617.0	1995	60.53	0.418	516.81	35,58
17	188.2	896.19	1639.3	2004	60.83	0.424	525.07	35,86
18	191.8	913.33	1672.3	2004	61.52	0.439	542	36,5
19	197.7	941.43	1709.7	1993	62.29	0.471	571.95	37,24
20	198.8	946.67	1719.5	2012	62.53	0.469	576.45	37,43
21	198	942.86	1698.3	1992	62.72	0.483	583.07	37,59
22	32.93	156.81	330.7	2496	40.51	0.047	129.28	14,96
23	42.81	203.86	446.4	2529	41.74	0.059	150.36	16,19
24	51.94	247.33	547.4	2499	43.65	0.075	172.49	18,11
25	61.05	290.71	643.2	2498	45.14	0.09	196.9	19,58
26	70.46	335.52	735.2	2493	46.71	0.106	222.87	21,11
27	80.99	385.67	843.0	2493	48.24	0.123	250.35	22,6
28	91.66	436.48	945.7	2508	49.83	0.139	279.69	24,17
29	103	490.48	1043.5	2483	51.47	0.161	310.69	25,79
30	120.7	574.76	1210.8	2518	54	0.188	360.44	28,28
31	139.3	663.33	1369.8	2501	56.62	0.224	413.77	30,87
32	160.2	762.86	1542.4	2488	59.2	0.265	471.13	33,41
33	180.7	860.48	1702.9	2456	61.68	0.315	532.17	35,84
34	186.5	888.1	1756.9	2493	62.6	0.321	552.15	36,69
35	192.4	916.19	1800.0	2473	63.45	0.341	574.57	37,52
36	199.1	948.1	1848.1	2457	64.16	0.361	595.71	38,21
37	203.8	970.48	1875.2	2458	64.91	0.376	617.53	38,93
38	206	980.95	1912.5	2509	65.41	0.374	631.44	39,41
39	206.9	985.24	1920.2	2517	65.44	0.377	636.33	39,43

experimental points that were predicted within a 20% error range, again for all combinations of void fraction and frictional loss correlations analyzed.

Table 3. Frictional Pressure Drop Correlations Performance-MAE

	Rouhani (1969)	Kanizawa and Ribatski (2016)	Tibiriçá <i>et al.</i> (2017)
Friedel (1979)	18.31%	16.79%	17.8%
Müller-Steinhagen and Heck (1986)	14.04%	12.61%	13.93%
Tibiriçá <i>et al.</i> (2017)	14.14%	10.78%	15.28%

The overall performance of all combinations was good and near. Differences in MAE were less than 10% when comparing the correlations. The correlation of Müller-Steinhagen and Heck (1986) has presented in general slightly

Table 4. Frictional Pressure Drop Correlations Performance-Convergency within 20% error

	Rouhani (1969)	Kanizawa and Ribatski (2016)	Tibiriçá <i>et al.</i> (2017)
Friedel (1979)	76.42%	82.05%	74.36%
Müller-Steinhagen and Heck (1986)	79.48%	87.18%	76.92
Tibiriçá <i>et al.</i> (2017)	71.79%	79.48%	71.79%

better results. However, the lowest MAE in all combinations was achieved using the pressure drop correlation of Tibiriçá *et al.* (2017) with the void fraction correlation of Kanizawa and Ribatski (2016). In this case, the MAE was 10.78%, and the convergence within the 10% margin of error was 79.48%. But the correlation of Müller-Steinhagen and Heck (1986), when also used with the void fraction given by Kanizawa and Ribatski (2016) obtained an MAE of 12.61%, very close to the one of Tibiriçá *et al.* (2017), and a better convergence of 87.18% within the 20% margin of error.

Figure 7 illustrates the comparison between predicted and experimental data for the 3 pressure drop correlations analyzed in the case where the void fraction of Kanizawa and Ribatski (2016) was used. It can be seen that, for an error range of 20%, all correlations obtained good and similar convergence. From Tab. 3 and 4, it is possible to see that the void fraction correlation used affected the predicted values of pressure drop and that slightly better results were obtained with the correlation of Kanizawa and Ribatski (2016).

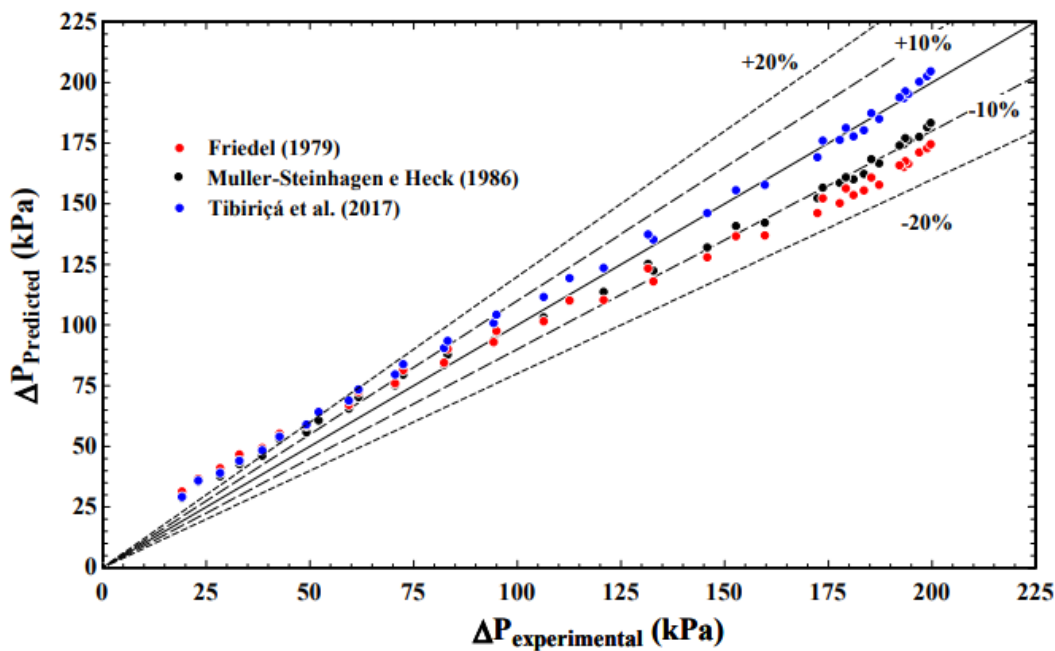


Figure 7. Comparison of predictive methods against the experimental data

6. CONCLUSIONS

New data on two-phase pressure drop in microchannels with R123 were obtained in this study. These data may be used to compare the pressure drop of R123 during flow boiling in microchannels with new low-pressure mixtures and fluids. Mass velocities of 2000 and 2500 kg/m² were used in a microchannel with 1.1 mm in diameter and a heated length of 100 mm. Heat flux varied from 109.1 to 636.3 kW/m². These data contribute to enriching data banks of pressure drop for R123 since very few data about two-phase pressure drop with R123 in microchannels are presented in the literature. Different correlations to predict two-phase frictional pressure drop and void fraction were tested in view of the experimental results. Combinations of void correlation and head loss were analyzed.

In general, the pressure drop correlations have presented similar and good results for the prediction of the experimental data in this paper. The lowest MAE in the pressure drop prediction, of 10.78%, was obtained when using the correlation of Kanizawa and Ribatski (2016) in the prediction of the void fraction and that of Tibiriçá *et al.* (2017) in predicting frictional pressure drop. The best data convergence within a 20% margin of error was obtained by combining the correlation of Müller-Steinhagen and Heck (1986) for pressure drop, with the correlation by Kanizawa and Ribatski (2016) for the void fraction. This combination had a convergence of 87.18%.

It was noted that the void fraction correlation also had an impact of up to 5% on the MAE of the prediction of the experimental data, so this is a point to be taken into account in the prediction of the two-phase pressure drop in microchannels, although many papers in the literature do not analyse the effect of different methods to predict the accelerational parcel.

7. ACKNOWLEDGEMENTS

The authors acknowledge FAPESP (grant 2019/11066-9 and 2021/10323-8, São Paulo Research Foundation), CAPES (Coordination for the Improvement of Higher Education Personnel, Finance Code 001), and CNPq (National Council for Scientific and Technological Development, process 304972/2017-7) for funding researches that have contributed to this study.

8. REFERENCES

- Chisholm, D., 1973. "Pressure gradients due to friction during the flow of evaporating two-phase mixtures in smooth tubes and channels". *Int. J. Heat Mass Transf.*, Vol. 16, pp. 347–358.
- Cicchitti, A., Lombardi, C., Silvestri, M., Soldaini, G. and Zavattarelli, R., 1960. "Two-phase cooling experiments: Pressure drop, heat transfer and burnout measurements". *Energia Nucleare*, Vol. 7, No. 4, pp. 407–425.
- Ennio, M. and Marco, A., 2017. "Organic rankine cycle (orc) power systems, technologies and applications". *WoodHead Publishing*.
- Friedel, L., 1979. "Improved friction pressure drop correlations for horizontal and vertical two phase pipe flow". *3R International*.
- Gardenghi, Á.R., dos Santos Filho, E., Chagas, D.G., Scagnolatto, G., Oliveira, R.M. and Tibiriçá, C.B., 2020. "Overview of void fraction measurement techniques, databases and correlations for two-phase flow in small diameter channels". *Fluids*, Vol. 5, No. 4, p. 216. doi:10.3390/fluids5040216.
- Hall, D. and Mudawar, I., 1999. "Ultra-high critical heat flux (CHF) for subcooled water flow boiling – ii: High-CHF database and design parameters". *Heat Mass Transfer*, Vol. 42, pp. 1429–1456.
- Hardik, B. and Prabhu, S., 2018. "Boiling pressure drop, local heat transfer distribution and critical heat flux in helical coils with r123". *International Journal of Thermal Sciences*, Vol. 125, pp. 149–165.
- Kandlikar, S.G., 2010. "Scale effects on flow boiling heat transfer in microchannels: A fundamental perspective". *International Journal of Thermal Sciences*, Vol. 49, No. 7, pp. 1073–1085. doi:10.1016/j.ijthermalsci.2009.12.016.
- Kanizawa, F.T. and Ribatski, G., 2016. "Void fraction predictive method based on the minimum kinetic energy". *Journal of the Brazilian Society of Mechanical Sciences and Engineering*, Vol. 38, No. 1, pp. 209–225. doi:10.1007/s40430-015-0446-x.
- Kanizawa, F.T. and Ribatski, G., 2021. *Flow boiling and condensation in microscale channels*. Springer International Publishing. doi:10.1007/978-3-030-68704-5.
- Kim, S.M. and Mudawar, I., 2014. "Review of databases and predictive methods for pressure drop in adiabatic, condensing and boiling mini/micro-channel flows". *International Journal of Heat and Mass Transfer*, Vol. 77, pp. 74–97. doi: 10.1016/j.ijheatmasstransfer.2014.04.035.
- Klein, A. and Alvarado, F., 2020. "EES - Engineering Equation Solver User's Manual". *FChart Software*, Vol. V.10.834-3D.
- Lockhart, R.W. and Martinelli, R.C., 1949. "Proposed correlation of data for isothermal two-phase, two-component flow in pipes". *Chem. Eng. Prog.*, Vol. 45, pp. 39–48.
- Lombaard, L., Moghimi, M.A., Valluri, P. and Meyer, J.P., 2021. "Interaction between multiple bubbles in microchannel flow boiling and the effects on heat transfer". *International Communications in Heat and Mass Transfer*.
- Müller-Steinhagen, H. and Heck, K., 1986. "A simple friction pressure drop correlation for two-phase flow in pipes". *Chemical Engineering and Processing: Process Intensification*, Vol. 20, No. 6, pp. 297–308. doi:10.1016/0255-2701(86)80008-3.
- Okajima, J., Jeong, S. and Maruyama, S., 2018. "Evaluation of cooling performance of ultrafine cryoprobes: Effect of probe structure on thermodynamic properties of refrigerant". *International Journal of Air-Conditioning and Refrigeration*, Vol. 26, No. 02, p. 1850020. doi:10.1142/s2010132518500207.
- Pang, K.C., Chen, S.C., Hung, T.C., Feng, Y.Q., Yang, S.C., Wong, K.W. and Lin, J.R., 2017. "Experimental study on organic rankine cycle utilizing r245fa, r123 and their mixtures to investigate the maximum power generation from low-grade heat". *Energy*, Vol. 133, No. 1, pp. 636–651.
- Quibén, J.M. and Thome, J.R., 2007. "Flow pattern based two-phase frictional pressure drop model for horizontal tubes, part ii: New phenomenological model". *International Journal of Heat and Fluid Flow*, Vol. 28, No. 5, pp. 1060–1072.
- Ribatski, G., Wojtan, L. and Thome, J., 2006. "An analysis of experimental data and prediction methods for two-phase frictional pressure drop and flow boiling heat transfer in microscale channels". *Exp. Therm. Fluid Sci.*, Vol. 31, pp. 1–19.

- Roldão, T.C.B., Brasil, J.S. and Tibiriçá, C.B., 2022. “Record heat flux for flow boiling of r123 in a single microchannel”. In *Proceedings of the 19th Brazilian Congress of Thermal Sciences and Engineering - ENCIT 2022*. ABCM - Brazilian Society of Mechanical Sciences and Engineering, Bento Gonçalves, RS, Brazil.
- Rouhani, S.Z., 1969. “Modified correlations for void-fraction and pressure drop”. . *AB Atomenergi Sweden, AE-RTV-841*, pp. 1–10.
- Tank, P.N., Hardik, B.K., Sridharan, A. and Prabhu, S.V., 2021. “Pressure drop, local heat transfer coefficient, and critical heat flux of dnb type for flow boiling in a horizontal straight tube with r-123”. *Heat and Mass Transfer*, Vol. 57, pp. 223–250. doi:<https://doi.org/10.1007/s00231-020-02935-5>.
- Tibiriçá, C.B., Rocha, D.M., Sueth, I.L.S., Bochio, G., Shimizu, G.K.K., Barbosa, M.C. and dos Santos Ferreira, S., 2017. “A complete set of simple and optimized correlations for microchannel flow boiling and two-phase flow applications”. *Applied Thermal Engineering*, Vol. 126, pp. 774–795. doi:10.1016/j.applthermaleng.2017.07.161.
- Zuber, N. and Findlay, J., 1965. “Average volumetric concentration in two-phase flow systems”. *Journal of Heat Transfer*, Vol. 87, No. 4, pp. 453–468.

9. RESPONSIBILITY NOTICE

The authors are solely responsible for the printed material included in this paper.